JOURNAL OF APPLIED ELECTROCHEMISTRY 25 (1995) 208–211

A novel miniature zirconia gas sensor with pseudo-reference
Part III: Simple implementation for the determination of air-to-fuel ratio

M. BENAMMAR*, W. C. MASKELL

Energy Technology Centre, Middlesex University, Bounds Green Road, London N11 2NQ, Great Britain

Received 22 December 1993

A novel mode of operation of a double-chamber zirconia oxygen sensor is presented. A pseudo-reference gas was generated in one chamber of the sensor to pin the potentials of the electrodes acting to pump oxygen to or from the other chamber. The circuitry was simple and readily implemented. The sensor was tested in the flue of a gas-burning system and shown to provide an output which enabled the normalized air-to-fuel ratio, λ, to be measured over the range $0.7 < \lambda < 1.7$. The characteristics are discussed from a theoretical standpoint.

1. Introduction

It is well known [1–3] that the single-chamber amperometric zirconia oxygen sensor, when operated in the flue gases of a combustion system, does not enable unambiguous determination of the air-to-fuel ratio (A/F) on both sides of stoichiometry. The reasons for this have been clarified recently [4]. Operation of the sensor with the anode in a reference gas (e.g., air) solves this problem by pinning the potential of this electrode [1, 5–9]. An attractive modification
of this idea is to replace the reference gas with a pseudo-reference gas (PRG) generated by electrochemical oxygen pumping. This may be achieved by adding a second chamber, to contain the PRG, to the sensor [10]. The sensor can then be sited away from walls separating the flue gases from air with the advantage to the system designer of increased flexibility.

There are several possible modes of operation of the sensor with a pseudo-reference [10], two of which were discussed recently [4, 11]. In this paper a third mode is described which has the advantage of simplicity of implementation while still enabling A/F to be determined unambiguously on both sides of stoichiometry.

2. Experimental details

Apart from the circuitry, details were as previously provided [4]; the sensor was similar also so that characteristics were expected to be comparable between papers. The block diagram of the circuit used is shown in Fig. 1. A complication with the previous arrangements [4, 11], which was avoided here, was the need to leave circuits floating to avoid short circuiting. A constant current source supplied a current, I_B, to pump oxygen continuously into the pseudo-reference chamber B via electrodes 5 and 6. A constant voltage supply was applied to electrodes 3 and 4, the positive pole of the supply being connected to the latter; this acted to pump oxygen from chamber A to chamber B (or vice versa). Electrodes 1 and 2 were optional, not being essential for normal operation, and provided a gauge for monitoring the Nernstian e.m.f. between electrodes 1 and 2.

3. Results

Characteristics of the instrument are shown in Figs. 2 and 3. The variable parameters were the current, I_B, applied to the electrodes 5 and 6, the pumping voltage between electrodes 3 and 4 and the normalized A/F, λ.

The convention used regarding the signs of currents was that a positive current I_A pumped oxygen out of chamber A (and of course into chamber B) while a positive current I_B pumped oxygen out of chamber B (into the external gas). Thus the total current pumping oxygen into chamber B was $I_A - I_B$. As the purpose of I_B was only to pump oxygen into chamber B its sign was always negative.

4. Discussion

4.1. *Practical considerations*

The characteristic in Fig. 2(a) relating to a current I_B of -3 mA and an applied pump voltage of 500 mV shows that the sensor provided an unambiguous

*Present address: Department de Physique, Institut Preparative aux Etudes d'Igenieur de Nateul, 8000 Nateul, Tunisia.

0021-891X

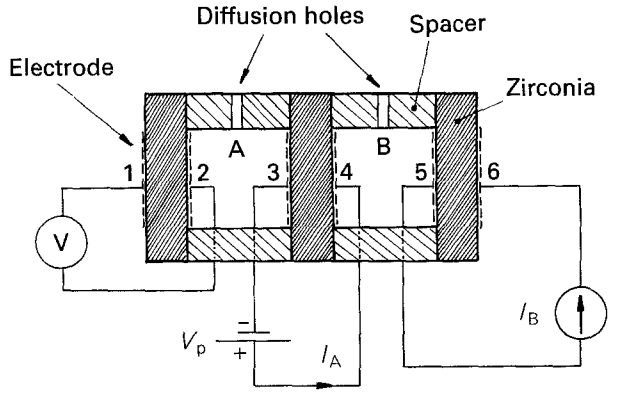

Fig. 1. Schematic diagram of the amperometric air-to-fuel ratio sensor with pseudo-reference obtained by continuous electrochemical pumping of oxygen into chamber B. The gauge (electrodes 1 and 2) included in chamber A is not essential for operation of the sensor.

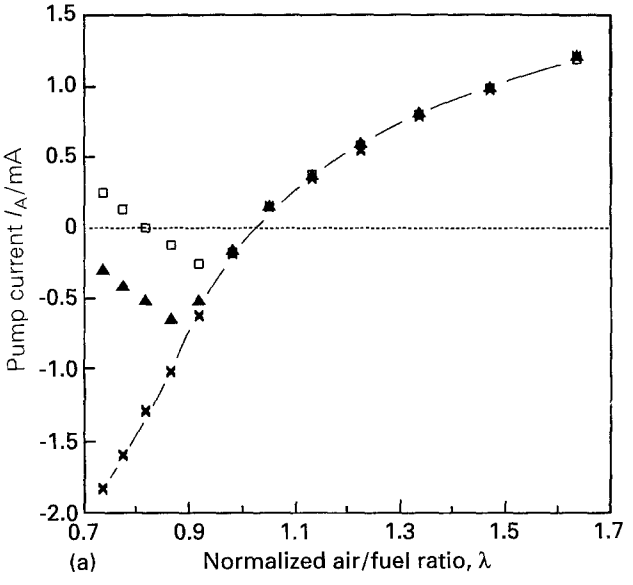

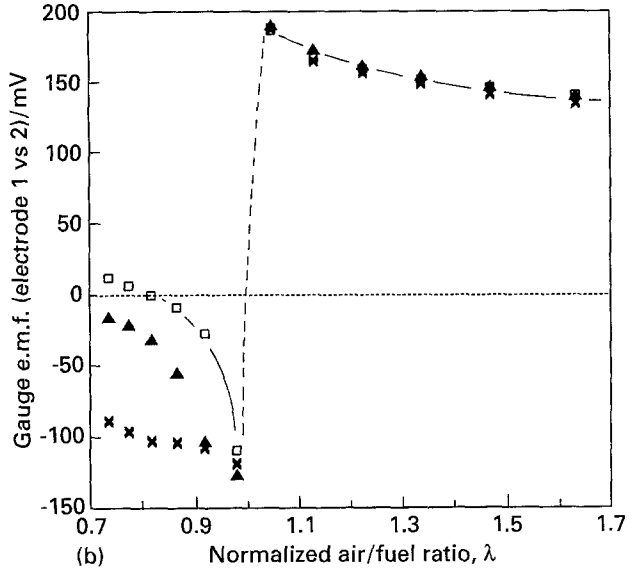

Fig. 2. Characteristics of the double-chamber device for various normalized air-to-fuel ratios (λ, λ = actual air-to-fuel ratio/stoichiometric air-to-fuel ratio). (a) Pump current, I_A, flowing between electrodes 3 and 4; (b) Nernstian e.m.f., E, between electrodes 1 and 2. The pump voltage, V_P, and operating temperature were 500 mV and 700° C, respectively. I_B: (×) −3.0, (▲) −1.0 and (□) −0.5 mA.

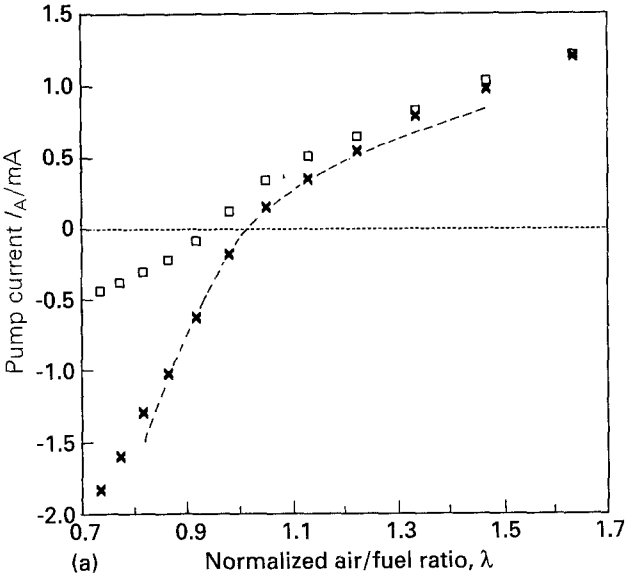

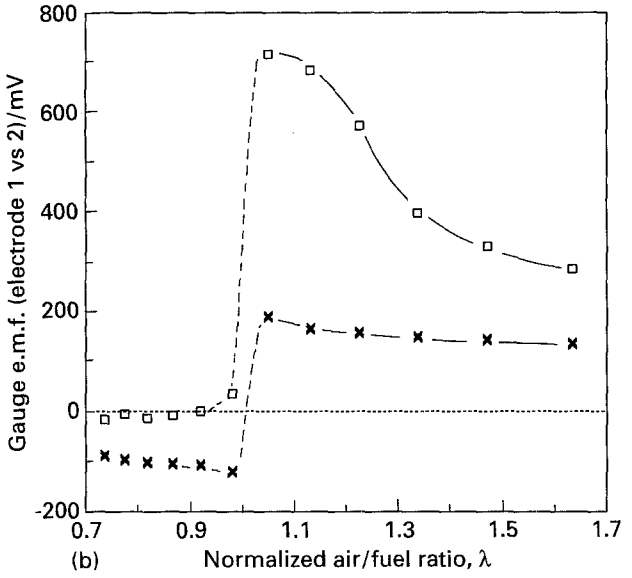

Fig. 3. Characteristics of the double-chamber device for various normalized air-to-fuel ratios (λ). The broken line in (a) shows the characteristic from Fig. 9 (for $I_B = -400\,\mu A$) of Part I [4]. (a) Pump current, I_A, flowing between electrodes 3 and 4; (b) Nernstian e.m.f., E, between electrodes 1 and 2. The current, I_B, and operating temperature were −3 mA and 700° C, respectively. V_P: (×) 500 and (□) 900 mV.

output current I_A for monitoring λ; this characteristic will be termed the standard characteristic. Comparison in Fig. 3(a) with the result from Part I [4] (data from Fig. 9 for $I_B = -400\,\mu A$) reveals that the characteristics in the two modes were almost identical. This finding is satisfying as the implementation described in this paper was substantially simpler than that in Part I.

Reduction of the magnitude of I_B to −1.0 and −0.5 mA provided characteristics which were almost identical for $\lambda > 1$ but different for $\lambda < 1$.

The effect of increasing the applied pump voltage, V_P from 500 to 900 mV (Fig. 3(a)), was to modify the characteristic so that it no longer matched the standard characteristic. In particular, the output current I_A was substantially greater than zero at stoichiometry ($\lambda = 1$). In practice this is undesirable as it is normally important to be able readily to identify the stoichiometric point. From a practical

standpoint, to monitor a system on both sides of stoichiometry, the magnitudes of I_B and V_P should be chosen so as to generate the standard characteristic over the possible range of λ of the combustion system. Deviations from this standard characteristic are discussed in the following Section.

4.2. *Theoretical considerations*

4.2.1. Excess air ($\lambda > 1$); pump voltage, $V_P = 0.5\,V$. The behaviour on the excess air side of stoichiometry ($\lambda > 1$) was straightforward. Reactions at electrodes 3–6 were as follows:

$$O_2 + 4e^- \underset{4,5}{\overset{3,6}{\rightleftharpoons}} 2O^{2-} \qquad (1)$$

Thus the effect of each current, I_A and I_B, was to pump oxygen into chamber B. As a result, for $\lambda > 1$, chamber B always contained excess oxygen ($\lambda_B > 1$, where λ_B represents the effective normalized A/F of the gas within chamber B). Clearly also $\lambda_B > \lambda > 1$; in this situation the gas within chamber B provided a satisfactory pseudo-reference as an electrode within that gas maintained a sufficiently stable reference potential (±50 mV, see Fig. 4) to which the potentials of the electrodes 3 and 4 were pinned. Furthermore, oxygen was being electrochemically pumped out of chamber A via electrode 3 (Equation 1) and simultaneously diffusing into A through the hole connecting that chamber to the sample gas. As a result there was an oxygen concentration difference between electrodes 1 and 2 generating a Nernstian e.m.f., E, where

$$E = \frac{RT}{4F}\ln\left(\frac{P}{P_A}\right) \qquad (2)$$

shown in Fig. 2(b). P and P_A are the oxygen partial pressures in the sample gas and within chamber A respectively. R, T and F have their usual significance. Hence E took positive values as shown in Fig. 2(b) for $\lambda > 1$. At 700° C Equation 2 indicates that E should change by approximately 50 mV per decade ratio of P to P_A. Thus the 150–200 mV e.m.f. shown in Fig. 2(b) for $\lambda > 1$ indicates that P_A was 3–4 orders of magnitudes lower than P, which is typical for an amperometric sensor operating in the limiting current plateau region [12].

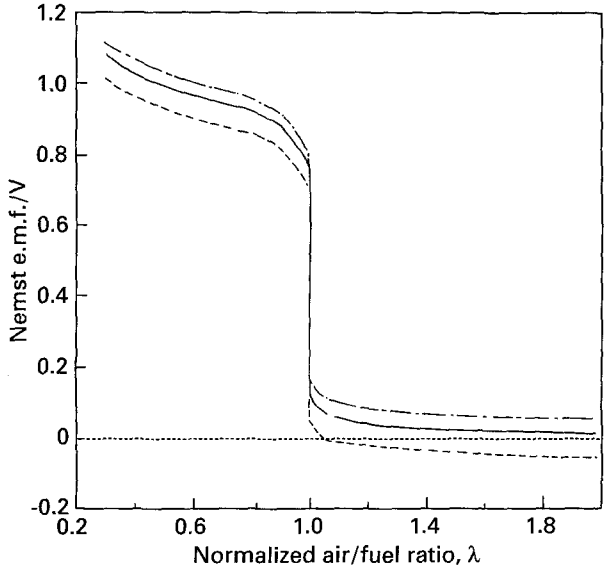

Fig. 4. Theoretical curves showing the Nernstian e.m.f. of a potentiometric cell operated at 750° C against normalized air-to-fuel ratio for combustion of methane in air [11]. Values for the reference oxygen partial pressure are: (–·–) 100, (——) 21 and (– – –) 1 kPa.

4.2.2. Excess fuel ($\lambda < 1$); pump voltage, $V_P = 0.5\,V$; operating on the standard characteristic. When the combustion system was operated with excess fuel ($\lambda < 1$) the situation was more complex. Figure 2(a) shows that the current I_A then took negative values; I_B was always negative and the magnitude of the total current pumping oxygen into chamber B, $I_A - I_B$, decreased as the magnitude of I_A increased. However, for the standard characteristic the composition of the gas within chamber B contained free oxygen ($\lambda_B > 1$). Reactions at electrodes 5 and 6 were

$$CO_2 + 2e^- \underset{5}{\overset{6}{\rightleftharpoons}} CO + O^{2-} \qquad (3)$$

Current I_B over and above that required to oxidize all the CO diffusing into chamber B generated the excess oxygen as follows:

$$O_2 + 4e^- \underset{5}{\longleftarrow} 2O^{2-} \qquad (1a)$$

In that circumstance ($\lambda_B > 1$) the gas within B provided a satisfactory pseudo-reference against which to pin the potentials of electrodes 3 and 4 (Fig. 4).

The current I_A was negative and this was pumping oxygen into chamber A via electrodes 3 and 4 according to

$$O_2 + 4e^- \xrightarrow{4} 2O^{2-} \qquad (1b)$$

and

$$CO_2 + 2e^- \underset{3}{\longleftarrow} CO + O^{2-} \qquad (3a)$$

However, while operating on the standard characteristic the composition of gas in chamber A remained substoichiometric, i.e. contained free CO and no free O_2, ($\lambda_A < 1$, where λ_A represents the effective normalized A/F of the gas within chamber A). Clearly also $\lambda_A > \lambda$ ($E > 0$, see Fig. 3(b)); the crucial point to note here is that a Nernstian e.m.f. was generated between electrodes 3 and 4 with a value around 800 mV (Fig. 4) but in the opposite sense to the applied voltage, V_P. As a result the net pumping voltage was changed from a value of 500 mV pumping oxygen from A to B, to a value of around 300 mV pumping oxygen from B to A. Thus it is clear why the current I_A switched sign from positive to negative as λ moved in the negative direction through the stoichiometric point ($\lambda = 1$).

λ_A was greater than λ because oxygen was being pumped into chamber A by current I_A: but also $\lambda_A < 1$ and $\lambda < 1$. As a result a Nernstian e.m.f. was generated between electrodes 1 and 2 with electrode 1 negative with respect to 2. Thus, there was a change

in sign of E as stoichiometry was traversed (Fig. 2(b)). In the substoichiometric region ($\lambda < 1$) the e.m.f. observed of approximately −100 mV was in line with expectation (Fig. 4).

4.2.3. Excess fuel ($\lambda < 1$); pump voltage, $V_P = 0.5$ V; not operating on the standard characteristic. It was found (Fig. 2(a)) that as λ decreased progressively below unity the characteristic deviated from the standard characteristic for I_B values of −0.5 and −1.0 mA. From considerations in Part I [4] it may be deduced that the deviation occurred when the gas in chamber B no longer provided a satisfactory pseudo-reference. In general terms this may be understood as follows. As λ decreased so the concentration of CO in the sample gas increased as too did the rate of diffusion of CO into chamber B. The current to oxidize the CO to CO_2 (Equation 3(a)) was $I_A - I_B$, which was progressively decreasing. Eventually a point was reached (for $I_B = -0.5$ or −1.0 mA) where the current, $I_A - I_B$, was only just sufficient to oxidize all the CO diffusing into chamber B. At that point $\lambda_B = 1$ and the potential of an electrode within chamber B moved by several hundred millivolts for very small deviations in λ_B from unity; likewise the back e.m.f. between electrodes 3 and 4 was very sensitive to these deviations and decreased as the potential of electrode 4 moved to more positive values. As a result the net voltage pumping oxygen from chamber B to A decreased with a consequential decrease in I_A. Thus, it is clear why the characteristic deviated from the standard characteristic as λ decreased if the magnitude of I_B was small.

4.2.4. Excess air ($\lambda > 1$); pump voltage, $V_P = 0.9$ V. When the pumping voltage, V_P, was increased from 500 to 900 mV current I_A moved to more positive values (Fig. 3(a)). Clearly at the higher pumping voltage the processes occurring at electrode 3 were firstly

$$O_2 + 4e^- \xrightarrow{3} 2O^{2-} \qquad (1c)$$

and additionally

$$CO_2 + 2e^- \xrightarrow{3} CO + O^{2-} \qquad (3b)$$

The current enhancement was due to Reaction 3(b) which was the result of the application of the additional 400 mV to the pump via electrodes 3 and 4. Reaction 3(b) generated a CO/CO_2 mixture within chamber A so that $\lambda_A < 1$ while $\lambda > 1$ (in the excess air region) and $\lambda_B > 1$. This explains the observed gauge e.m.f. of around 700 mV shown in Fig. 3b and expected from Fig. 4.

4.2.5. Stoichiometry ($\lambda = 1$); pump voltage, $V_P = 0.9$ V. At stoichiometry there was negligible oxygen in the gas surrounding the sensor and so Reaction 1(c) was no longer significant. However, Reaction 3(b) still proceeded to generate the positive value of I_A observed (Fig. 3(a)).

4.2.6. Excess fuel ($\lambda < 1$); pump voltage, $V_P = 0.9$ V. As stoichiometry was traversed towards lower λ values ($0.95 < \lambda < 1$), λ_B remained greater than 1 (excess in air in B) while λ_A decreased further until at $\lambda \approx 0.95$ the Nernstian e.m.f. between electrodes 3 and 4 approached 900 mV (Fig. 4); on reaching 900 mV ($0.90 < \lambda < 0.95$) the net pumping voltage was zero with a zero resultant pump current, I_A (Fig. 3(a)). When I_A was zero, $\lambda_A = \lambda$ and the gauge e.m.f. was zero (Fig. 3(b)).

Further reduction in λ ($\lambda < 0.90$) also reduced λ_A so that the Nernstian e.m.f. between electrodes 3 and 4 exceeded 900 mV and the net pump voltage reversed sign to produce negative I_A values. λ_B remained greater than 1 for the conditions shown. The negative I_A values caused $\lambda_A > \lambda$ shown by negative though small values of the gauge e.m.f. (Fig. 3(b)).

5. Conclusion

The double-chamber sensor with pseudo-reference performed satisfactorily, providing an unambiguous measure of normalized A/F, λ, over the range $0.7 < \lambda < 1.7$. Electronic circuitry was simple and not complicated by the need for floating circuit blocks. Characteristics could be fully interpreted according to established theory.

References

[1] H. Dietz, *Solid State Ionics* **6** (1982) 175.
[2] R. C. Copcutt and W. C. Maskell, *ibid.* **53–56** (1992) 119.
[3] W. C. Maskell, *in* 'Techniques and Mechanisms in Gas Sensing' (edited by P. T. Moseley, J. O. W. Norris and D. E. Williams) Adam Hilger, Bristol (1991) pp. 1–45.
[4] M. Benammar and W. C. Maskell, *Appl. Phys.* **A57** (1993) 45.
[5] S. Soejima and S. Mase, SAE paper 850 378, International Congress and Exposition, Detroit, Michigan, Feb. (1985) pp. 53–59.
[6] W. C. Vassel, E. M. Logothetis and R. E. Hetrick, SAE paper 841 250, Passenger Car Meeting, Dearborn, Michigan (1984) pp. 1–7.
[7] E. M. Logothetis, W.C. Vassell, R. E. Hetrick and W. J. Kaiser, *Sensors and Actuators* **9** (1986) 363.
[8] T. Sasayama, S. Suzuki, M. Ohsuga and S. Ueno, *Ceram. Eng. Sci. Proc.* **8** (1987) 1074.
[9] S. Ueno, N. Ichikawa, S. Suzuki and K. Terakado, SAE paper 860 409 (1987).
[10] W. C. Maskell, 1991, *UK Patent 2 208 007.*
[11] M. Benammar and W. C. Maskell, *in* 'Sensors VI: Technology, Systems and Applications' (edited by K. T. V. Grattan and A. T. Augousti), Institute of Physics Publishing, Bristol (1993) pp. 21–26.
[12] W. C. Maskell and B. C. H. Steele, *Solid State Ionics* **28–30** (1988) 1677.